Science Advances
AAAS

Supplementary Materials for

Organoid-on-a-chip model of human ARPKD reveals mechanosensing pathomechanisms for drug discovery

Ken Hiratsuka *et al.*

Corresponding author: Ryuji Morizane, rmorizane@mgh.harvard.edu, morizanr@da2.so-net.ne.jp; Jennifer A. Lewis, jalewis@seas.harvard.edu

Sci. Adv. **8**, eabq0866 (2022)
DOI: 10.1126/sciadv.abq0866

The PDF file includes:

Other Supplementary Material for this manuscript includes the following:

Supplementary Figures

Fig. S1

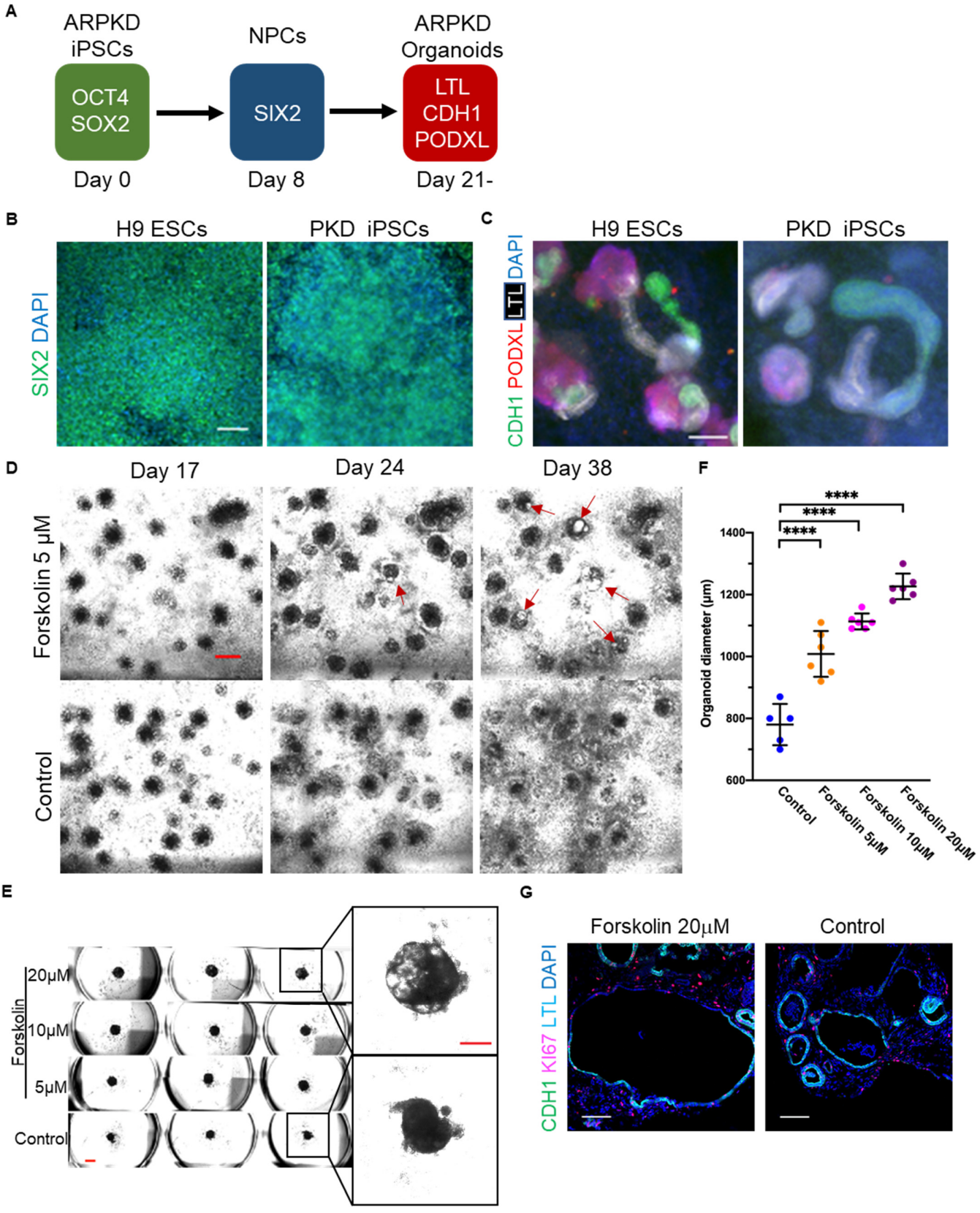

Fig. S1. ARPKD patient-derived organoids form cysts upon forskolin treatment. (A) Diagram of differentiation days. Markers for each step of differentiation are shown; OCT4 (POU class 5 homeobox 1), SOX2 (SRY-box), SIX2 (SIX2 homeobox 2), LTL (Lotus Tetragonolobus Lectin), CDH1 (Cadherin 1), and PODXL (Podocalyxin-like protein 1). (B) Immunocytochemistry for SIX2 on day 8 in cells differentiated from H9 ESCs and patient-derived iPSCs. Scale bars, 100 μm. (C) Immunocytochemistry for proximal tubule (LTL), distal tubule (CDH1), and podocyte (PODXL) in H9-derived 2D nephron formation and patient-derived 2D nephron formation on day 28. Scale bars, 200 μm. (D) Bright-field images of patient-derived 2D nephron structures treated with and without 5 μM forskolin on day 17, 24, and 38. Red arrows indicate cystic structures. Scale bars, 1 mm. (E) Bright-field images of patient-derived kidney organoids treated with and without forskolin (5 μM, 10 μM, and 20 μM) on day 23. Scale bar, 1 mm (left), 500 μm (right). (F) Organoid diameter in patient-derived organoids treated with and without forskolin (5 μM, 10 μM, and 20 μM) on day 23. (G) Immunocytochemistry for LTL, CDH1, and KI67 on day 51 in patient-derived organoids treated with 20 μM forskolin and control organoids. Scale bars, 100 μm. Values represent mean +/- s.d. **** represents $p < 0.0001$.

Fig. S2

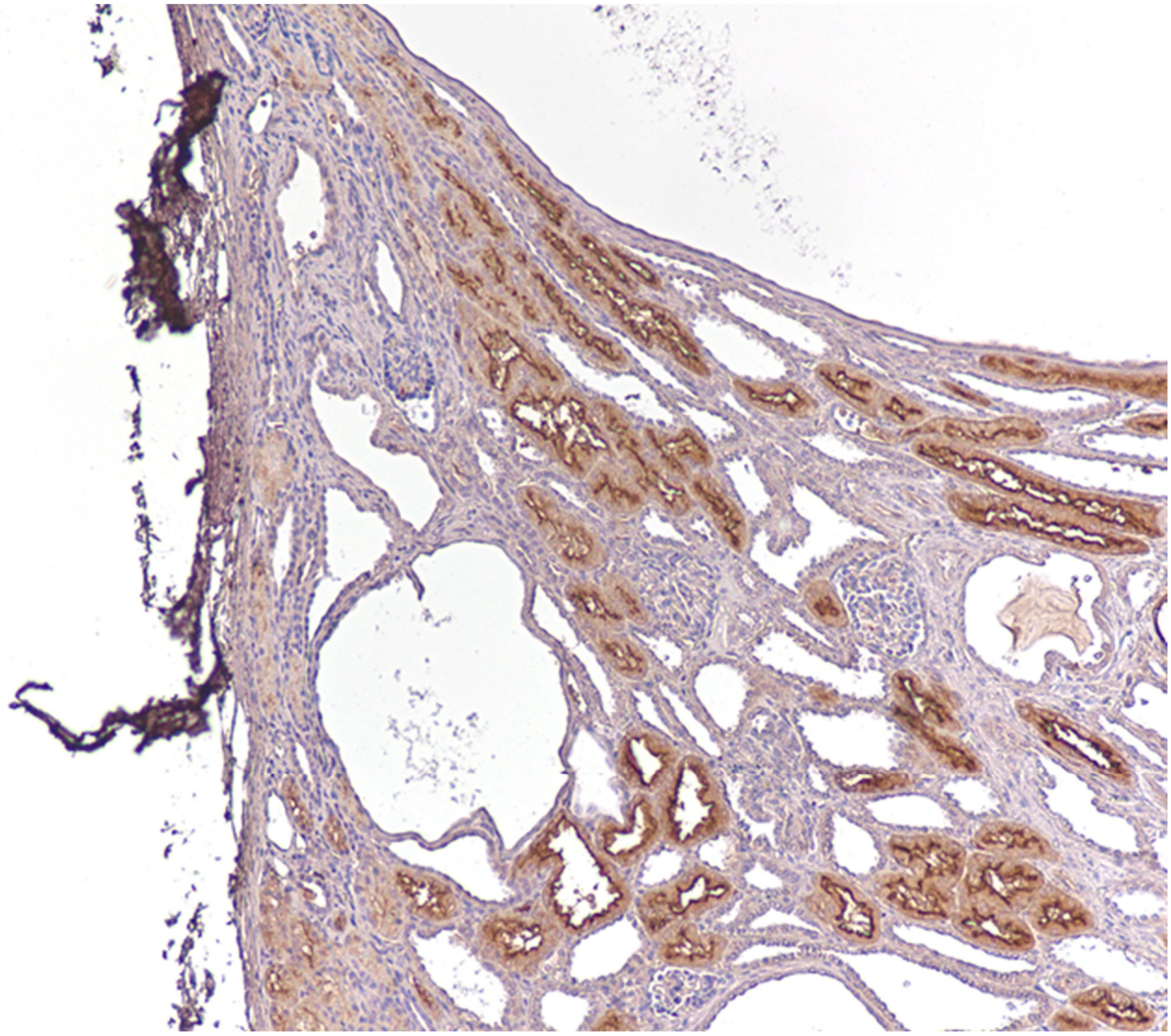

Fig. S2. Cysts in distal tubules in ARPKD sample (kidney cortex). A representative image of LTL staining in human kidney samples from ARPKD patients. Cysts are developed in LTL negative distal tubules in the kidney cortex. Asterisks indicate cysts. A scale bar: 100 μm.

Fig. S3

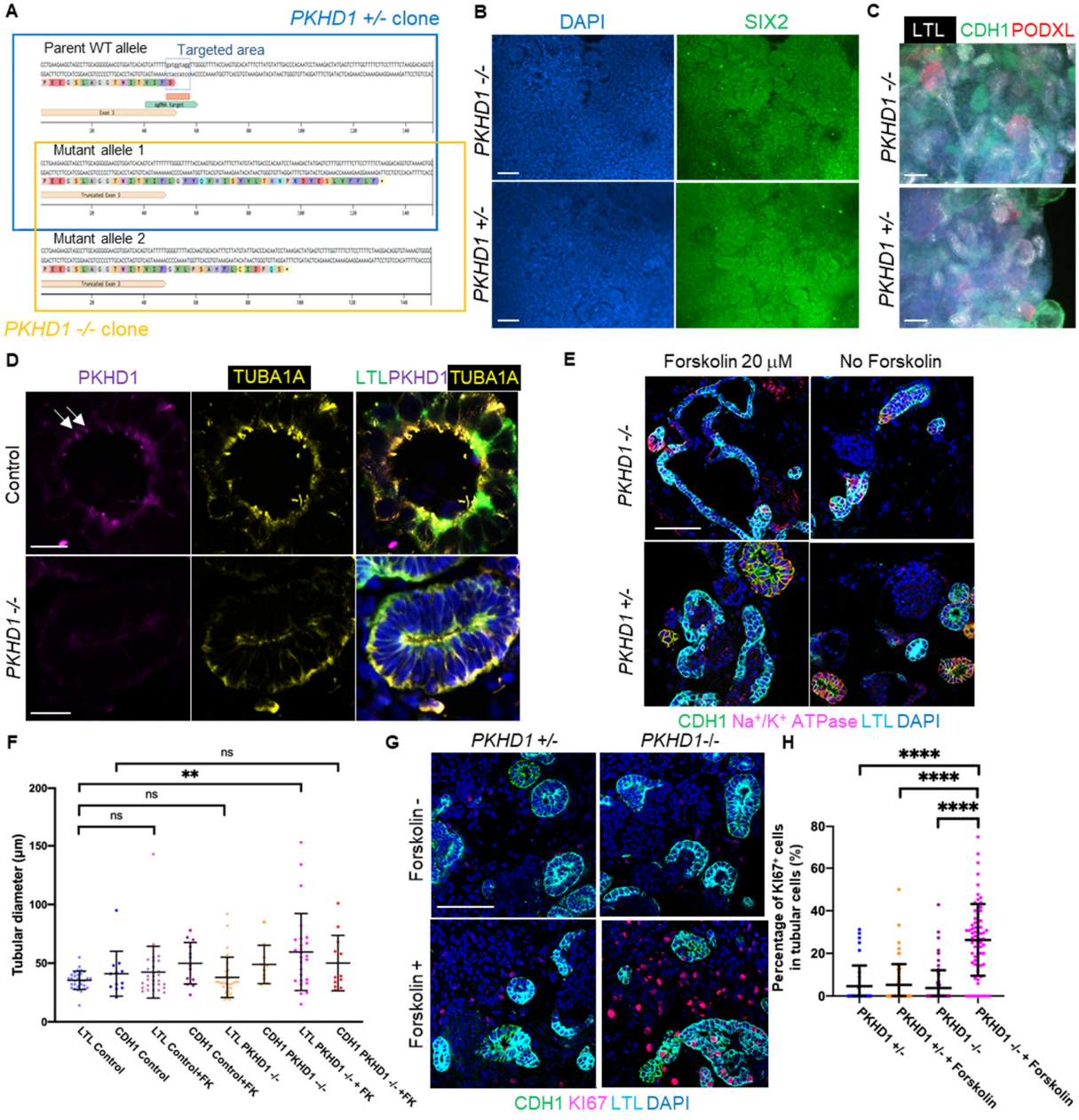

Fig. S3. *PKHD1-/-* organoids form cysts upon forskolin treatment. (A) Deep sequence of *PKHD1* gene in the mutant lines. 9 or 11 bases of nucleic acid were deleted at the exon-intron junction resulting in the translation termination soon after the mutation site. (B) Immunocytochemistry for SIX2 in *PKHD1-/-* and *PKHD1+/-* nephron progenitor cells on day 8. Scale bars, 100 μm. (C) Whole-mount immunostaining for proximal tubule (LTL), distal tubule (CDH1), and podocyte (PODXL) in *PKHD1-/-* and *PKHD1+/-* organoid on day 21. Scale bars, 100 μm. (D) Immunostaining for LTL, PKHD1 (arrows), and TUBA1A in control and *PKHD1-/-* organoid on day 35. Scale bar, 10 μm (upper), 20 μm (lower). (E) Immunocytochemistry for CDH1, Na^+/K^+ ATPase, and LTL in *PKHD1+/-* control and *PKHD1-/-* organoids with and without forskolin treatment on day 51. Scale bars, 100 μm. (F) Tubular diameter in *PKHD1+/-* (control) and *PKHD1-/-* organoids with and without forskolin (FK) 20 μM on day 51. (G) Immunostaining for KI67, CDH1, and LTL in *PKHD1+/-* control and *PKHD1-/-* organoids with and without forskolin on day 35. Scale bars, 100 μm. (H) Percentage of $KI67^+$ cells in *PKHD1+/-* and *PKHD1-/-* organoids with and without forskolin 20 μM on day 35. Values represent mean +/- s.d. ** represents $p < 0.01$, **** represents $p < 0.0001$.

Fig. S4

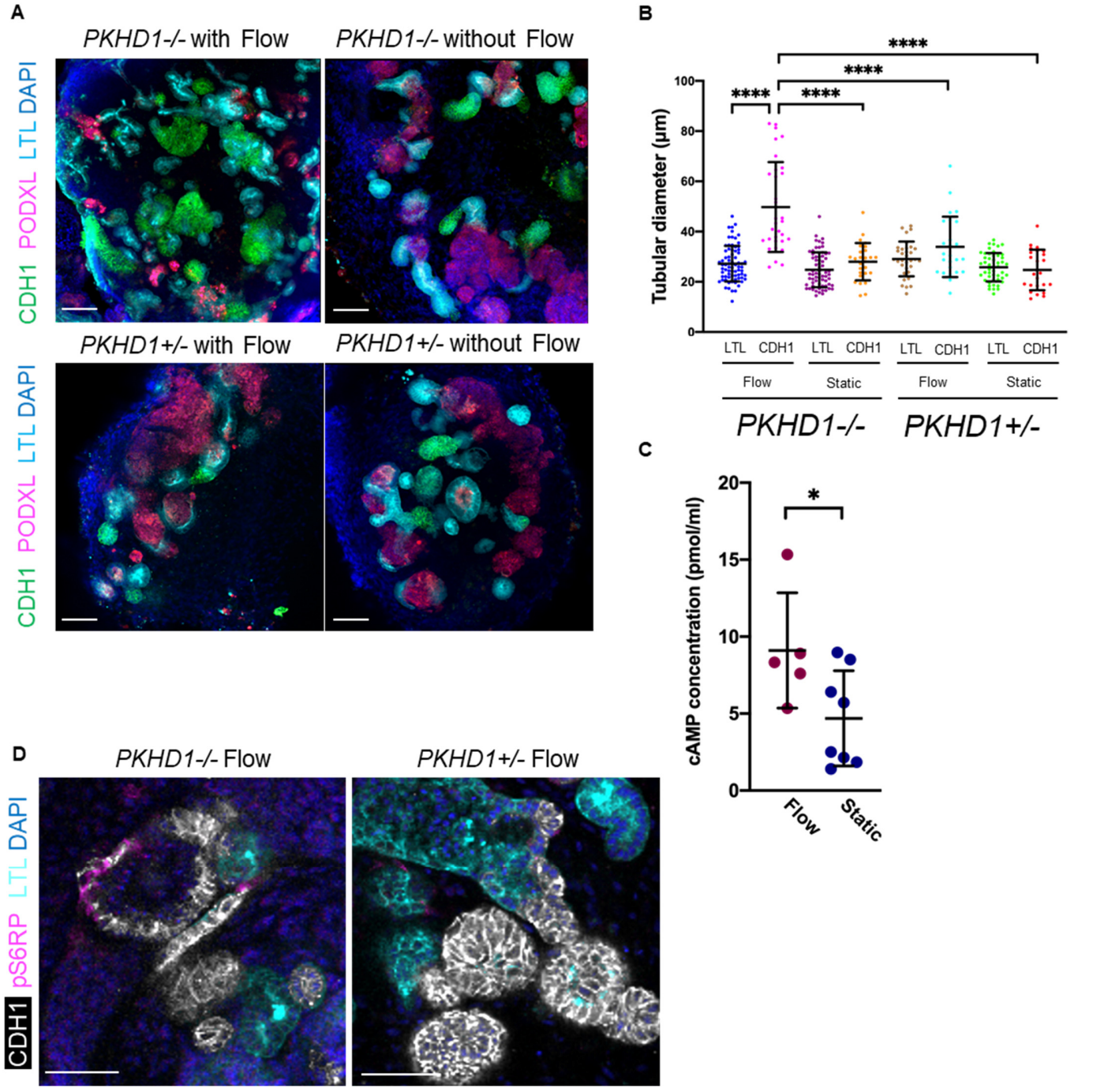

Fig. S4. Fluidic stress induces tubular dilatation in distal nephrons. (A) Whole-mount immunostaining for CDH1, PODXL, and LTL in *PKHD1-/-* and *PKHD1+/-* organoids with and without flow on day 35. Scale bar, 50 µm. (B) Tubular diameter in *PKHD1-/-* organoids with and without flow and *PKHD1+/-* organoids with and without flow on day 35. (C) cAMP concentration in *PKHD1-/-* organoids with and without flow (D) Whole-mount immunostaining for CDH1, pS6RP, and LTL in *PKHD1-/-* and *PKHD1+/-* organoids with flow on day 35. Scale bar, 50 µm. Values represent mean +/- s.d. Statistical significance for (B) was attributed to values of $P < 0.05$ as determined by one-way ANOVA with Tukey's multiple-comparisons test. For (C), statistical significance was attributed to values of $P < 0.05$ as determined by a Student's t-test. * represents $p < 0.05$ (c). **** represents $p < 0.0001$.

Fig. S5

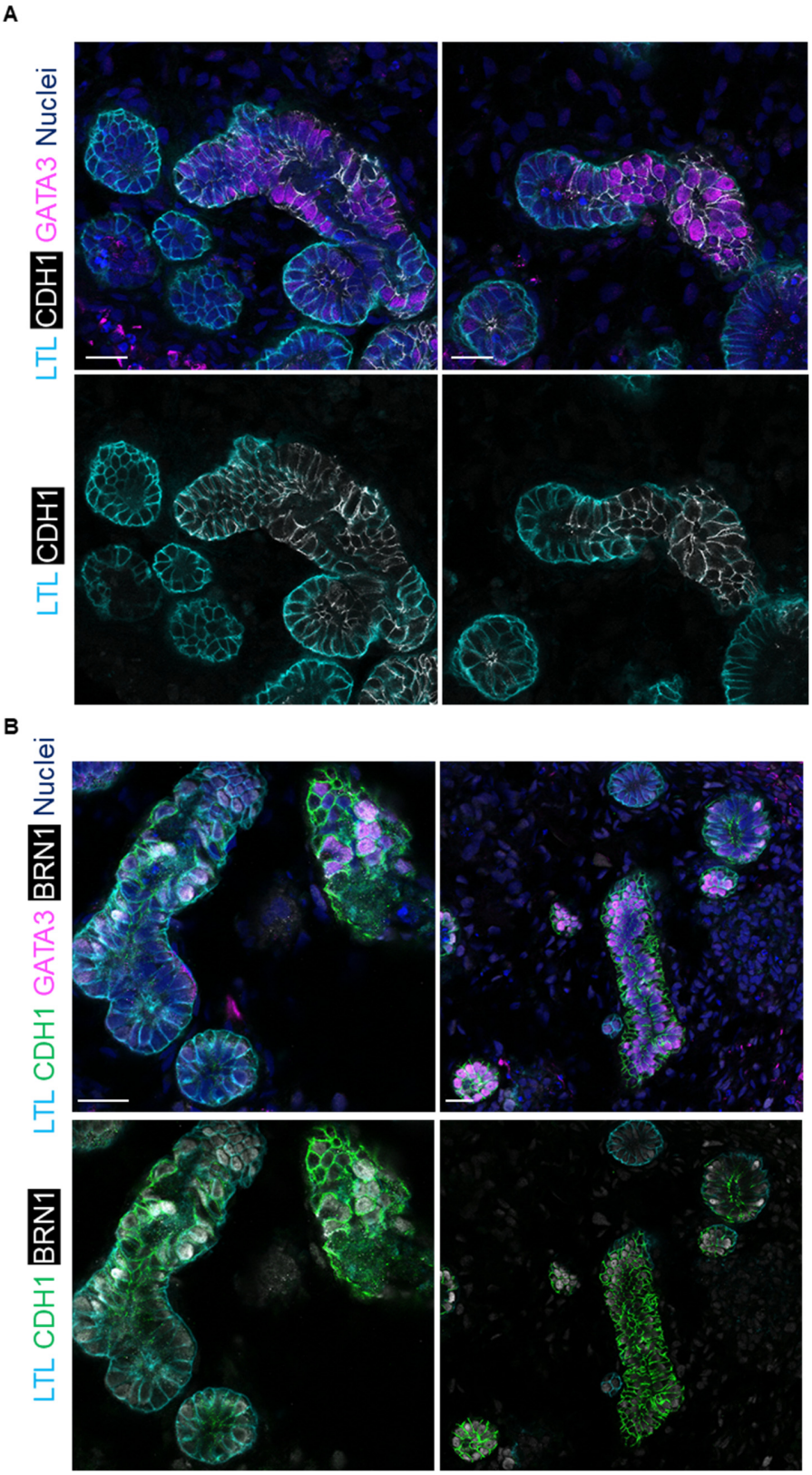

Fig. S5. Characterization of CDH1$^+$ distal nephrons. (A) Immunostaining for CDH1, GATA3, and LTL in H9 organoids on day 35 of differentiation. Scale bar, 20 μm. (B) Immunostaining for CDH1, GATA3, BRN1, and LTL in H9 organoids on day 35 of differentiation. Scale bar, 20 μm.

Fig. S6

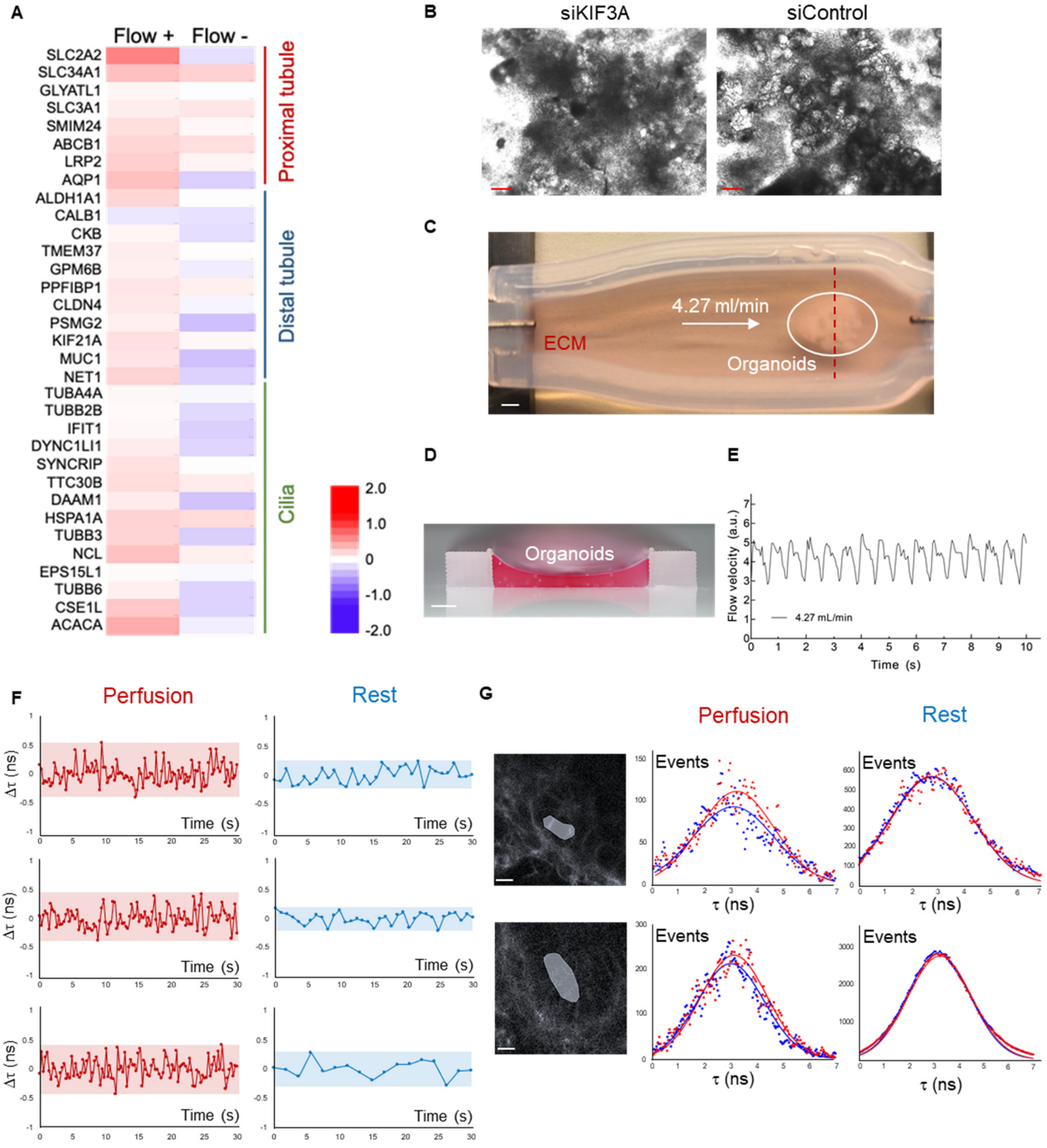

Fig. S6. Validation of ciliary signals and mechanosensing signals under flow. (A) Heat map of microarray datasets for proximal tubular markers (top), distal tubular markers (middle), and ciliary markers (bottom) in *PKHD1+/-* control organoids with and without flow on day 35 of differentiation. (B) Bright-field images of *PKHD1-/-* organoids transfected by siKIF3A and siControl on day 22. Scale bars, 200 μm. (C) A photograph of the millifluidic chip. White arrow highlights flow direction. White line indicates organoids on the chip. Fluidic shear stress in proximal tubules is estimated to vary between 0.7 and 1.0 dyn/cm^2. The flow rate at the beginning of the first proximal subsegment is equal to the glomerular filtration rate (120 ml/min) and the estimated flow rate

in the distal and collecting duct segment is 3-24 ml/min (1/5-1/40 of flow rate in the proximal segment), indicating 0.02-0.2 dyn/cm^2 in distal nephrons. Kidney organoids-on-chip serves FSS that ranges roughly 0.02-0.04 dyn/cm^2, suggesting physiologically relevant FSS in distal nephrons. Scale bars, 2 mm. (D) A photograph showing cross-sectional views (red dotted line in (C)) that highlight the location of organoids. Scale bars, 2 mm. (E) Flow-velocity measured at the center of the channel, 80 μm above the ECM surface, which reveals the pulsatile flow. (F) Lifetime change during perfusion (left) and rest (right) in other tubules. (G) Bright-field images of tubules in different organoids. The white area highlights the region where overall lifetimes and event counts were measured during perfusion and rest. Scale bar, 10 μm (left). Corresponding lifetime histograms during perfusion and rest (right).

Fig. S7

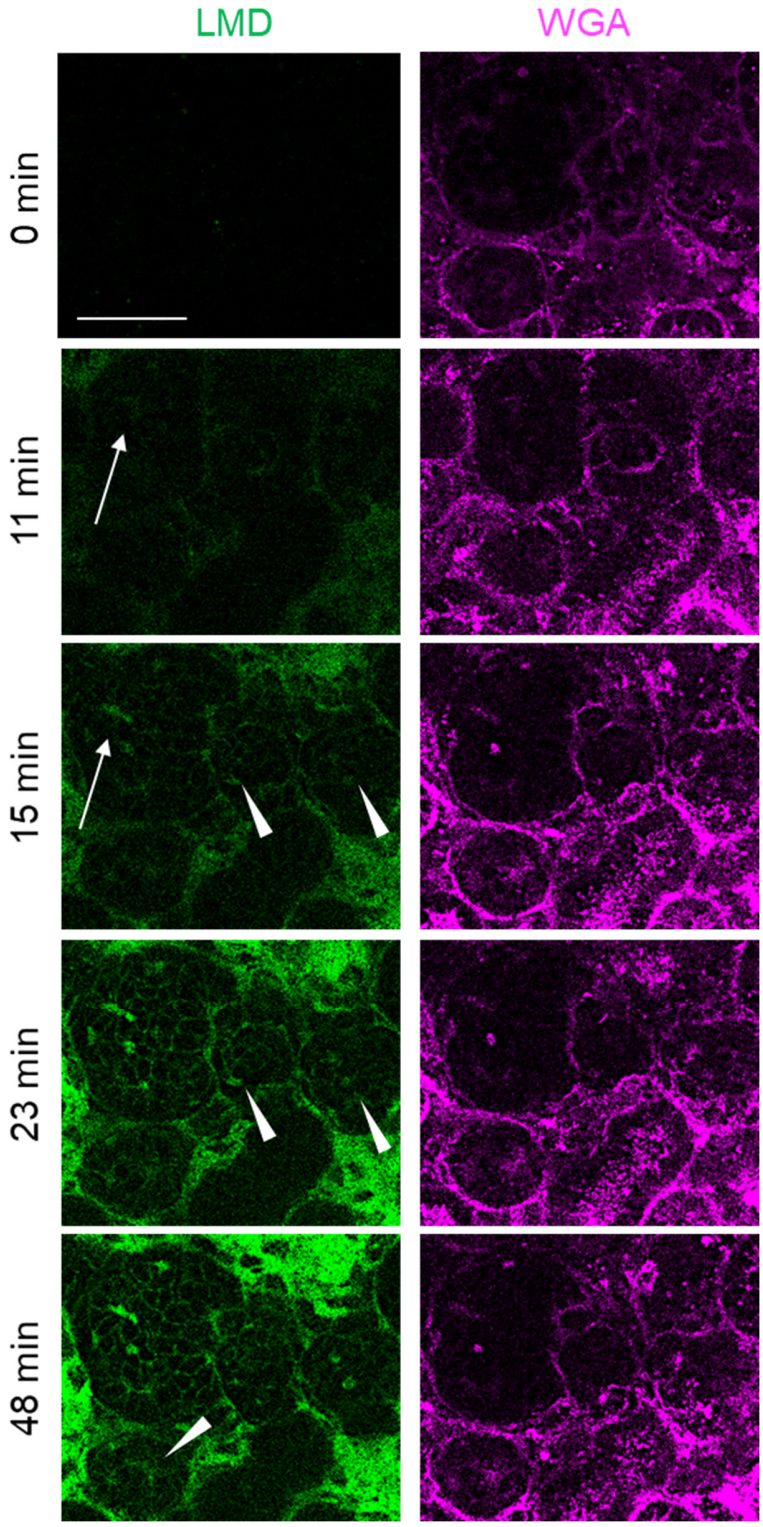

Fig. S7. Time-lapse images of LMD perfusion in live organoid cultured under flow. Live organoid images were taken at 0 min, 11 min, 15 min, 23 min, and 48 min after low-molecular weight dextran (LMD) was added to the medium reservoir. To avoid the chip oscillation caused by a peristaltic pump, the LMD medium was slowly perfused by gravity. Organoid epithelial structures were visualized by WGA staining before LMD perfusion. White arrows indicate LMD perfusion into glomerulus-like structures. White arrowheads indicate LMD perfusion into the tubular lumens. Scale bar, 50 μm

Fig. S8

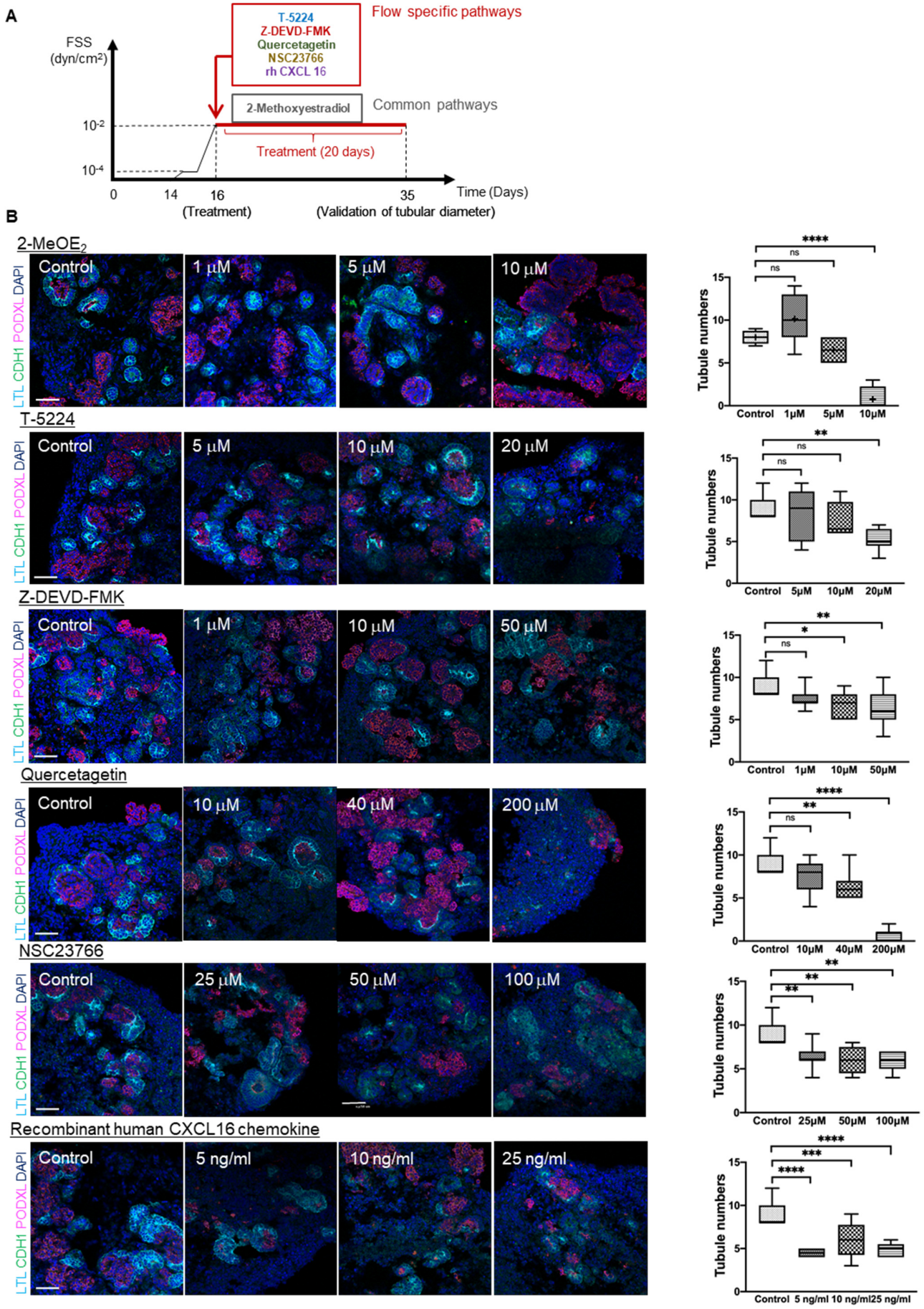
A
T-5224
Z-DEVD-FMK
Quercetagetin
NSC23766
rh CXCL 16
Flow specific pathways
2-Methoxyestradiol
Common pathways
FSS
(dyn/cm²)
10-2
10-4
Treatment (20 days)
0
14
16
35
Time (Days)
(Treatment)
(Validation of tubular diameter)
B
2-MeOE2
T-5224
Z-DEVD-FMK
Quercetagetin
NSC23766
Recombinant human CXCL16 chemokine
LTL CDH1 PODXL DAPI
Control
1 μM
5 μM
10 μM
20 μM
25 μM
40 μM
50 μM
100 μM
200 μM
5 ng/ml
10 ng/ml
25 ng/ml
Tubule numbers
ns
Control 1μM 5μM 10μM
Control 5μM 10μM 20μM
Control 1μM 10μM 50μM
Control 10μM 40μM 200μM
Control 25μM 50μM 100μM
Control 5 ng/ml 10 ng/ml 25 ng/ml

Fig. S8. Treatment of *PKHD1-/-* organoids with candidate compounds. (A) Schematic representation of time course to treat *PKHD1-/-* organoids with candidate compounds. (B) The evaluation of optimal concentration. Immunocytochemistry for proximal tubule (LTL), distal tubule (CDH1), and podocyte (PODXL) in *PKHD1-/-* organoids treated with 2-MeOE$_2$, T-5224, Z-DEVD-FMK, Quercetagetin, NSC23766, and rhCXCL16 chemokine at various concentrations from day 16 to 35 (left). Tubule numbers were counted on day 35 (right). Scale bars, 50 μm. Values represent mean +/- s.d. * represents $p < 0.05$ ** represents $p < 0.01$ *** represents $p < 0.001$ **** represents $p < 0.0001$.

Fig. S9

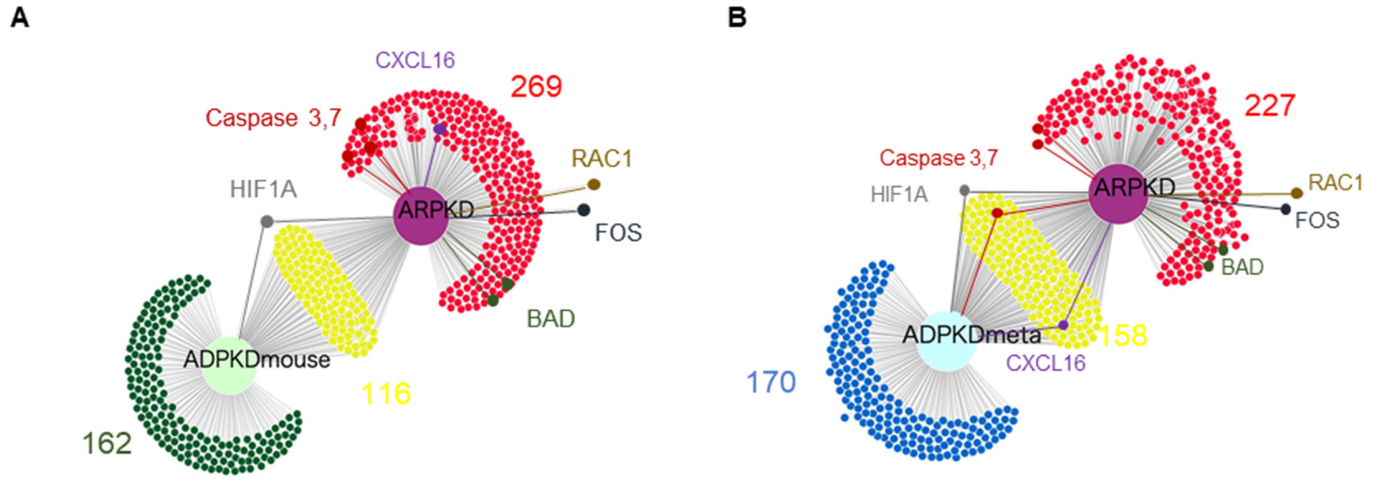

Fig. S9. DiVenn diagrams that compare pathways in our ARPKD model and publicly available ADPKD datasets. (A) A DiVenn diagram that compares pathways in our ARPKD model and mouse ADPKD dataset. (B) A DiVenn diagram that compares pathways in our ARPKD model and meta-analysis based ADPKD dataset. Meta- analysis was performed by combining available PKD expression profiling studies (mouse, rat, and human) and common DEGs were selected in mouse, rat, and human.

Fig. S10

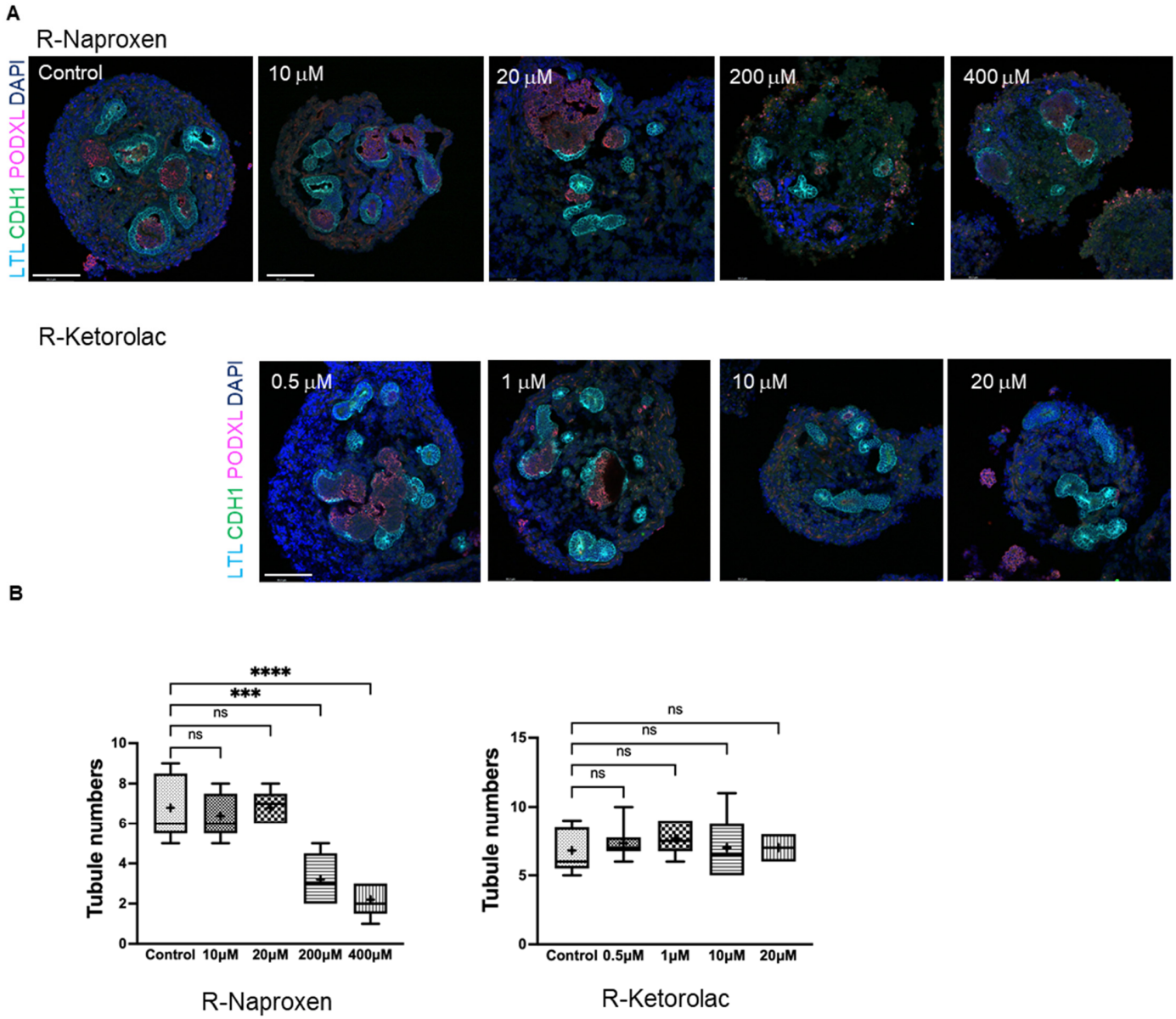

Fig. S10. The evaluation of optimal concentrations for R-Naproxen and R-Ketorolac treatment. (A) Immunostaining for proximal tubule (LTL), distal tubule (CDH1), and podocyte (PODXL) in *PKHD1-/-* organoids treated with R-Naproxen and R-Ketorolac at various concentrations from day 16 to 35. Scale bars, 100 μm. (B) Tubule numbers were counted on day 35. Values represent mean +/- s.d. *** represents $p < 0.001$ **** represents $p < 0.0001$.

Fig. S11

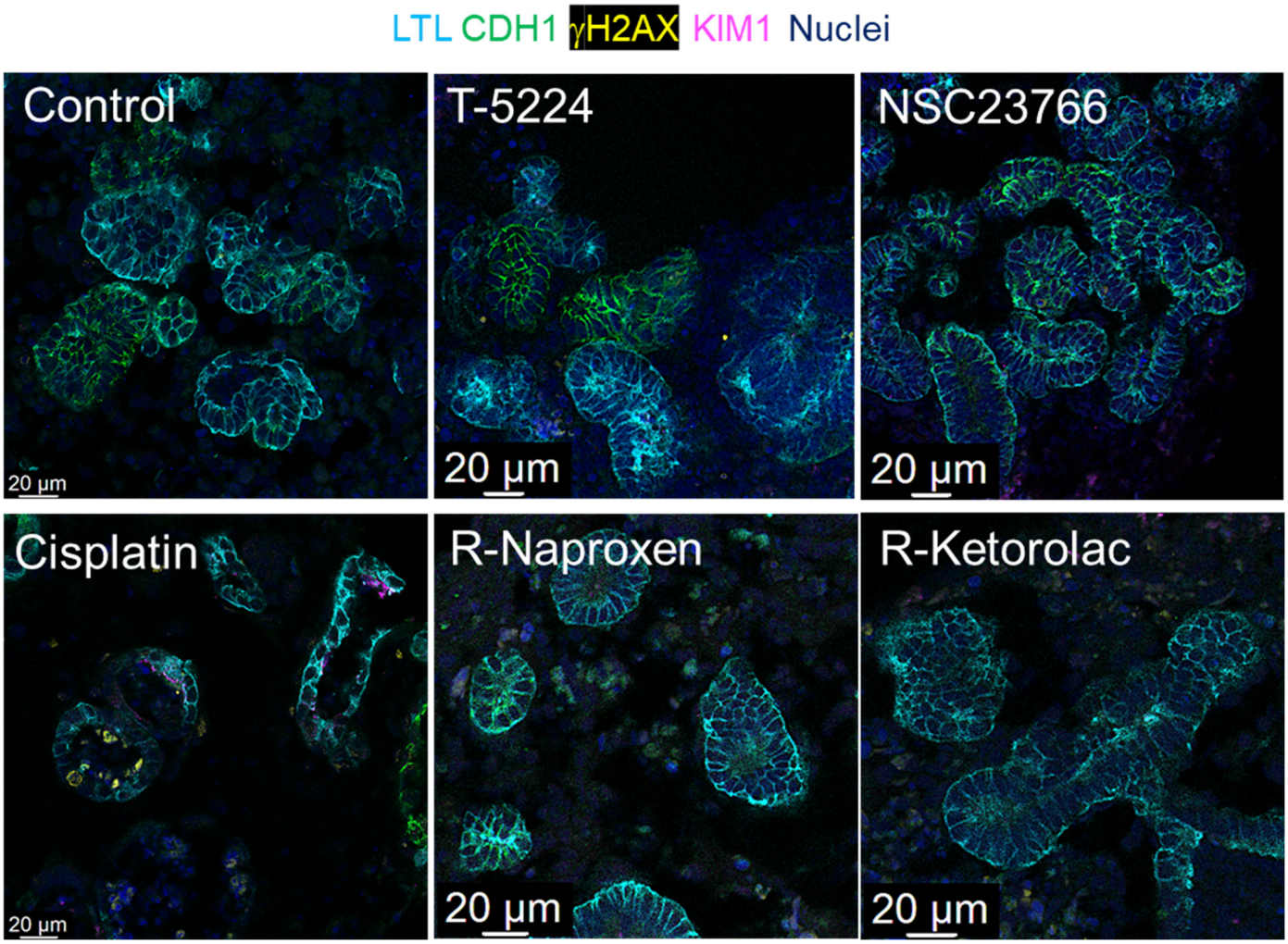

Fig. S11. Validation of tubular toxicity of candidate compounds in *PKHD1-/-* organoids. Immunostaining for proximal tubule (LTL), distal tubule (CDH1), KIM-1, and γH2AX in *PKHD1-/-* organoids treated with T-5224, NSC23766, R-Naproxen, and R-Ketorolac at the optimal concentration from day 16 to 35, and treated with 5 μm of cisplatin for one day as a positive control. Scale bars, 20 μm.

Fig. S12

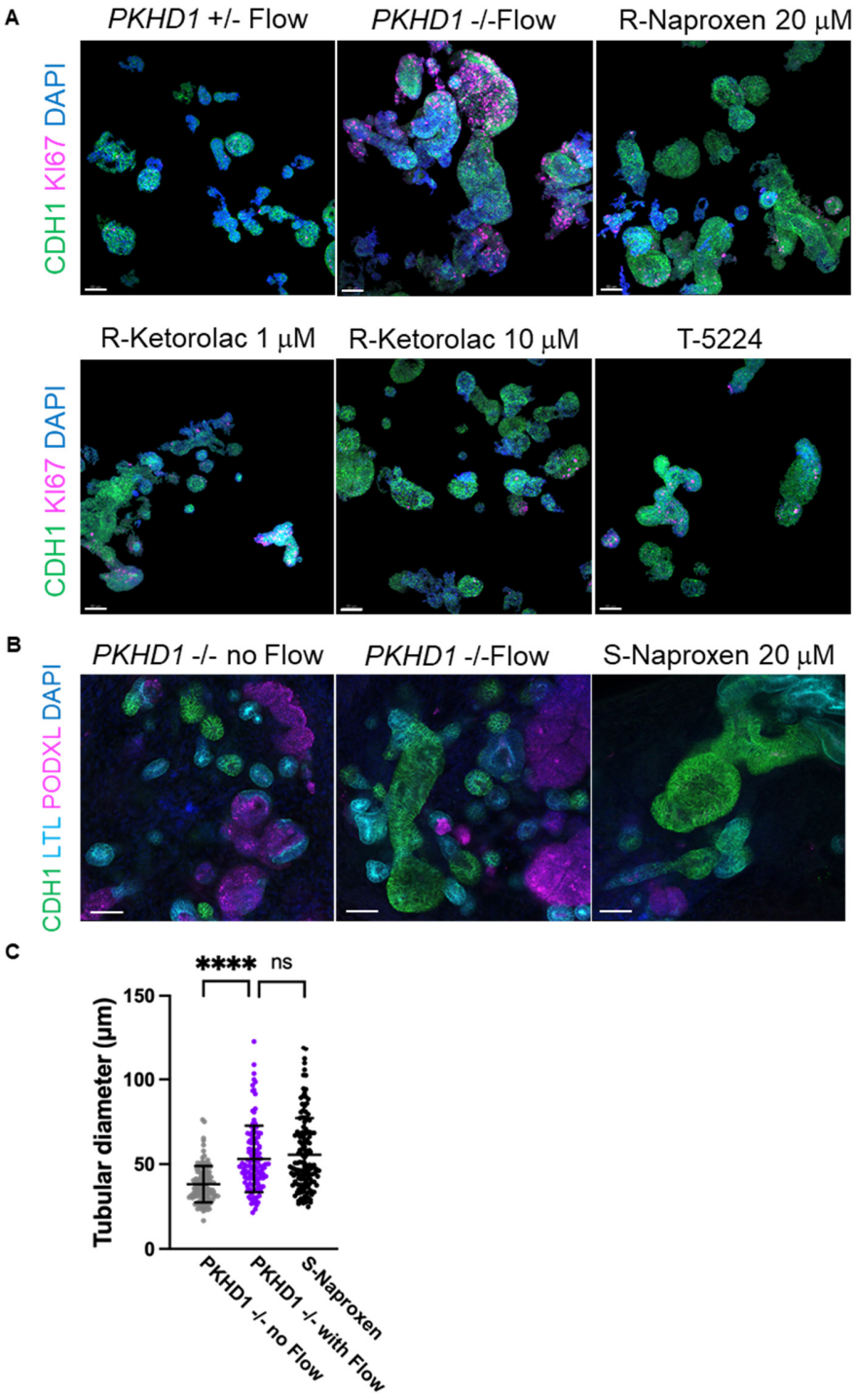

Fig. S12. 3D confocal imaging of whole organoids by z-stacks from top to bottom. (A) Whole-mount immunostaining for CDH1 and KI67 in *PKHD1*+/- organoids under flow and *PKHD1*-/- organoids treated with candidate drugs (R-Naproxen 20 μM, R-Ketorolac 1 μM, R-Ketorolac 10 μM, and T-5224 10 μM) under flow. Scale bars, 50 μm. (B) Whole-mount immunostaining for CDH1, LTL, and PODXL in *PKHD1*-/- organoids on day 35, cultured in three different conditions: 1. No flow, 2. Flow, and 3. Flow and S-Naproxen 20 μM. Scale bars, 50 μm. (C) A dot plot graph of tubular diameters in $CDH1^{+}$ tubules in *PKHD1*-/- organoids shown in figure S12B. Values represent mean +/- s.d. Statistical significance was attributed to values of $P < 0.05$ as determined by one-way ANOVA with Tukey's multiple-comparisons test. **** represents $p < 0.0001$.

Fig. S13

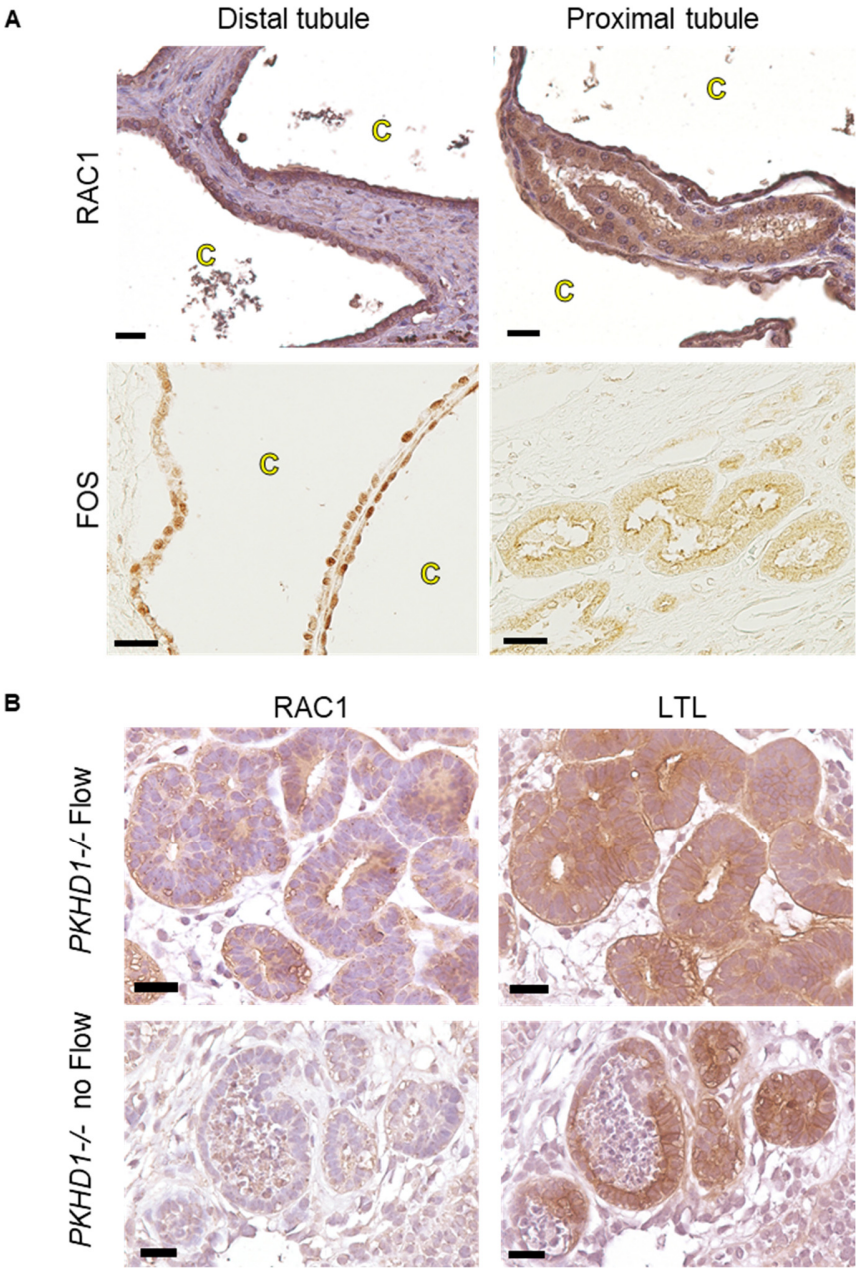

Fig. S13. RAC1 and FOS expression in human kidneys and *PKHD1-/-* organoids. (A) Immunostaining for RAC1 in cystic epithelial cells (upper left) and proximal tubule (upper right) in human kidney samples from patients with ARPKD. Immunostaining for FOS in cystic epithelial cells (lower left) and proximal tubule (lower right) in human kidney samples from patients with ARPKD. Scale bars 25 µm. (B) Immunostaining for RAC1 in proximal tubules in *PKHD1-/-* with and without flow on day 35 (left). Immunostaining for LTL in proximal tubules in *PKHD1-/-* with and without flow on day 35 (right). Scale bars 25 µm.

Fig. S14

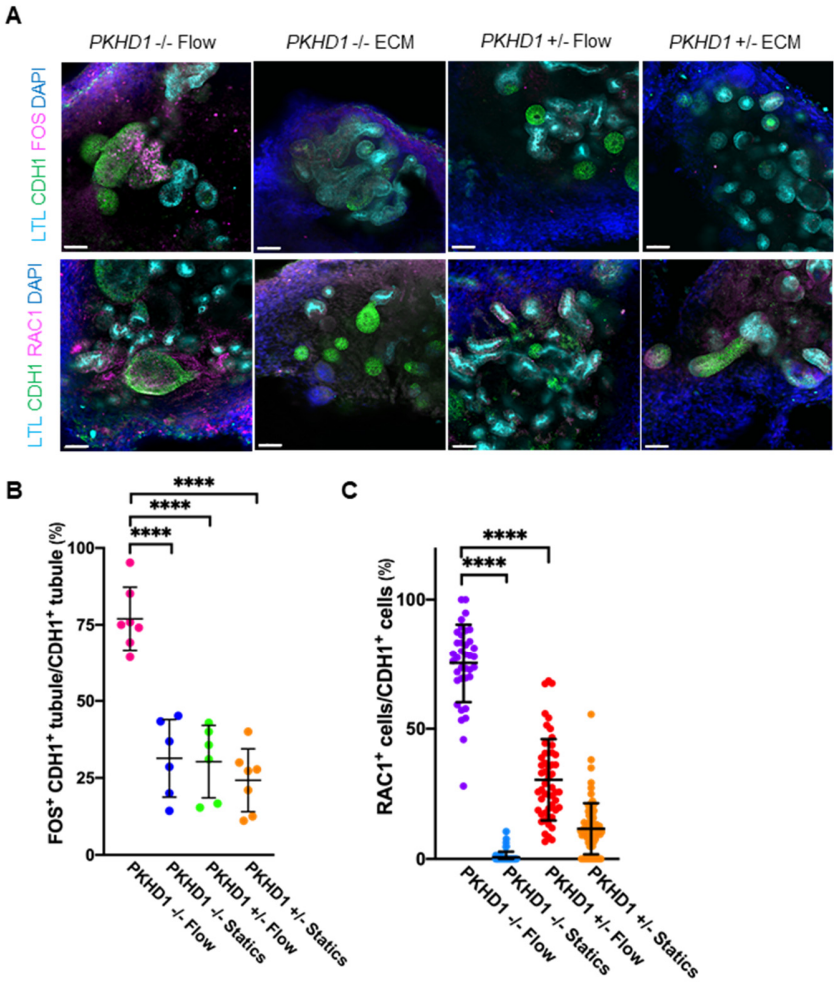

Fig. S14. Expression of FOS and RAC1 in *PKHD1*-mutant organoids with and without flow. (A) Immunostaining for FOS (upper), RAC1 (lower), LTL, and CDH1 in *PKHD1*-/- organoids with and without flow, and *PKHD1*+/- organoids with and without flow on day 35. Scale bars 50 μm. (B) Percentage of FOS^+ $CDH1^+$ tubules/$CDH1^+$ tubules in *PKHD1*-/- organoids with and without flow, and in *PKHD1*+/- organoids with and without flow on day 35. (C) Percentage of $RAC1^+$ cells in distal nephrons in *PKHD1*-/- organoids with and without flow, and in *PKHD1*+/- organoids with and without flow on day 35. Values represent mean +/- s.d. **** represents $p < 0.0001$.

Fig. S15

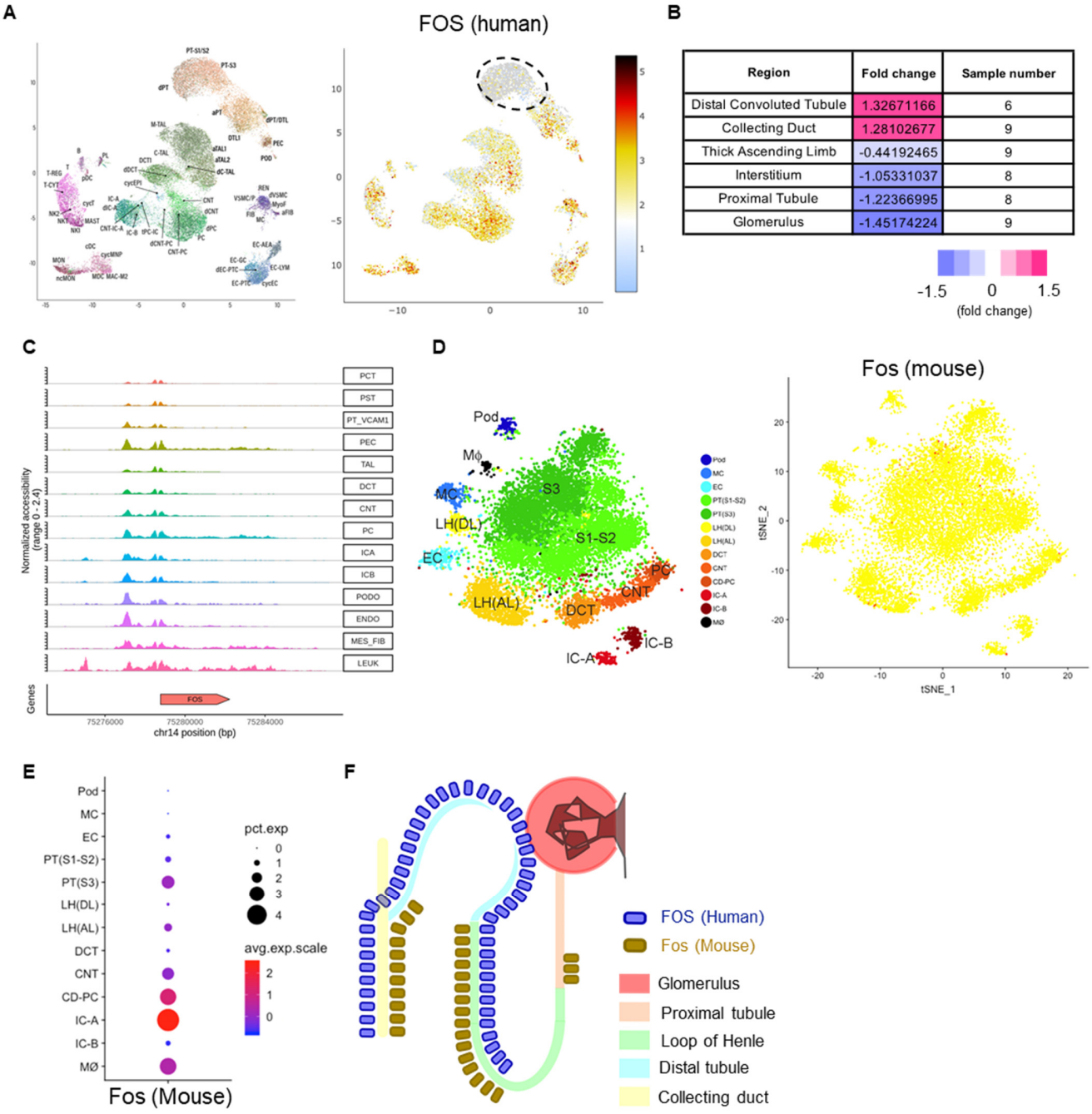

Region	Fold change	Sample number
Distal Convoluted Tubule	1.32671166	6
Collecting Duct	1.28102677	9
Thick Ascending Limb	-0.44192465	9
Interstitium	-1.05331037	8
Proximal Tubule	-1.22366995	8
Glomerulus	-1.45174224	9

Fig. S15. Transcriptome analysis confirms RAC1 and FOS expression in tubules under various conditions. (A) Visualization of single-cell transcriptomes in uniform manifold approximation and projection (UMAP) of datasets which is comprised of 20 samples from 18 living healthy donor biopsy participants (left). FOS expression in UMAP space from healthy donor biopsy participants (right). Dashed black line highlights proximal tubule clusters. (B) FOS gene expression comparison by the regional transcriptomics across regions in healthy kidney (HRT). (C) FOS chromatin accessibility profiles in human kidneys. Chromatin accessibility profiles showing genome tracts representing a region in chromosome 14 of human kidneys identifying 14 separate cell clusters (D) t-Distributed Stochastic Neighbor Embedding (t-SNE) plot of snRNA-seq dataset of healthy mouse kidney identifying 13 separate cell clusters (left). t-SNE plot displaying Fos gene expression (right). (E) Gene expression of Fos across clusters in the healthy mouse dataset. The original data of (A,B) and (C-E) are available at https://www.kpmp.org/ and http://humphreyslab.com/SingleCell/ respectively. (F) A schematic illustrating species difference in FOS/ Fos expression.

Fig. S16

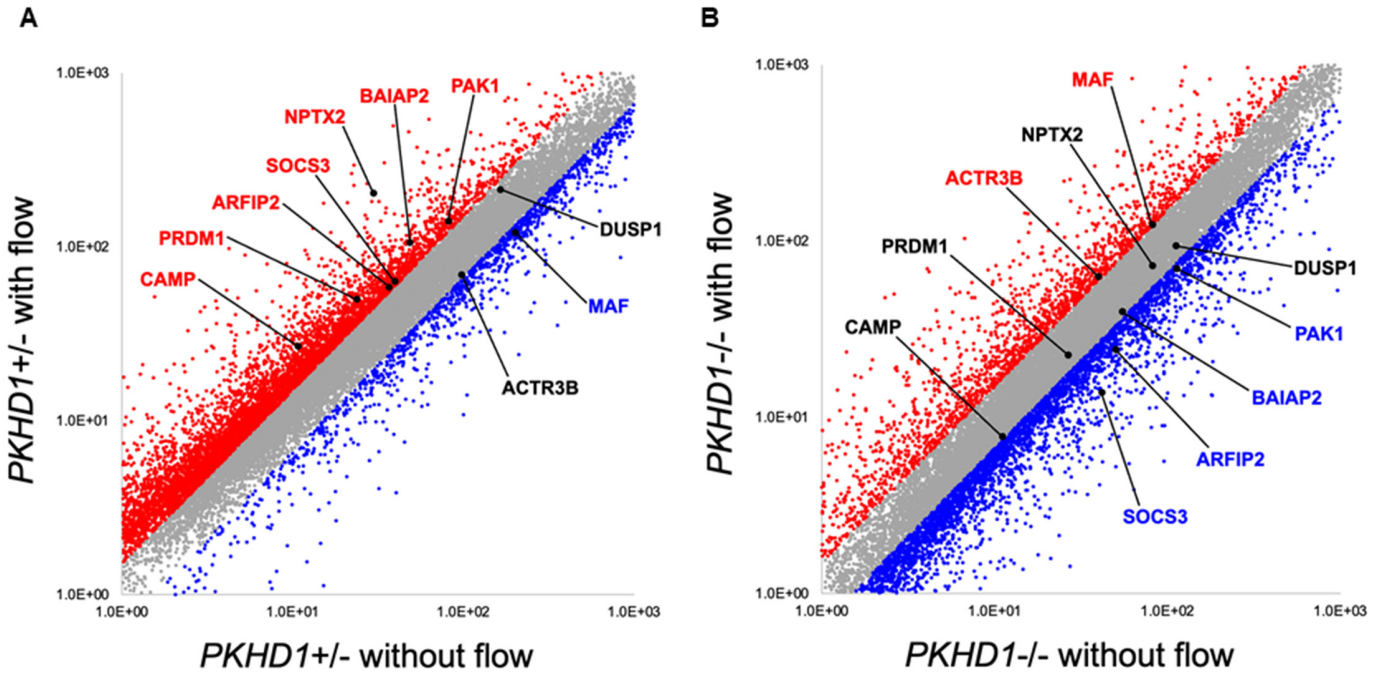

Fig. S16 *PKHD1-/-* mutant organoids exhibit altered gene regulation in response to flow. Scatter plots comparing expression profiles of flow and no flow culture in (A) *PKHD1*+/- (control) and (B) *PKHD1*-/- organoids. Red and blue dots represent genes with >1.5-fold upregulation and downregulation respectively when compared to no flow samples. Gene names associated with RAC1 and FOS pathways are shown in the scatter plots.

Fig. S17

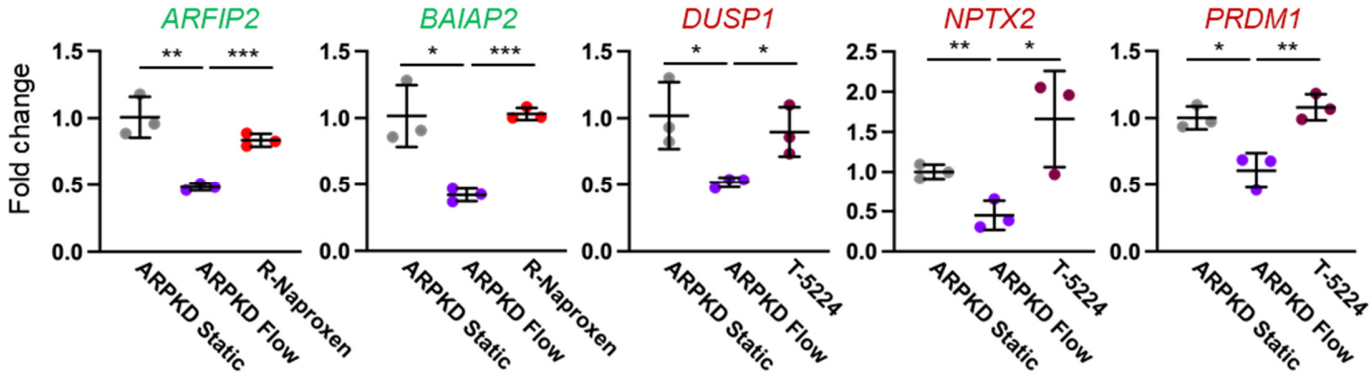

Fig. S17 Gene expression of RAC1 and FOS downstream genes. qPCR for RAC1 genes (ARFIP2 and BAIAP2) in green color and FOS genes (DUSP1, NPTX2, and PRDM1) in red color in ARPKD patient-derived organoids treated with R-Naproxen or T-5224 under flow conditions on day 23 of differentiation. Values are normalized against the control, ARPKD patient-derived organoids cultured in static conditions. Values shown are the means +/- s.d. p-values were determined by a Student's t-test. * represents $p < 0.05$; ** represents $p < 0.01$ *** represents $p < 0.001$.

Fig. S18

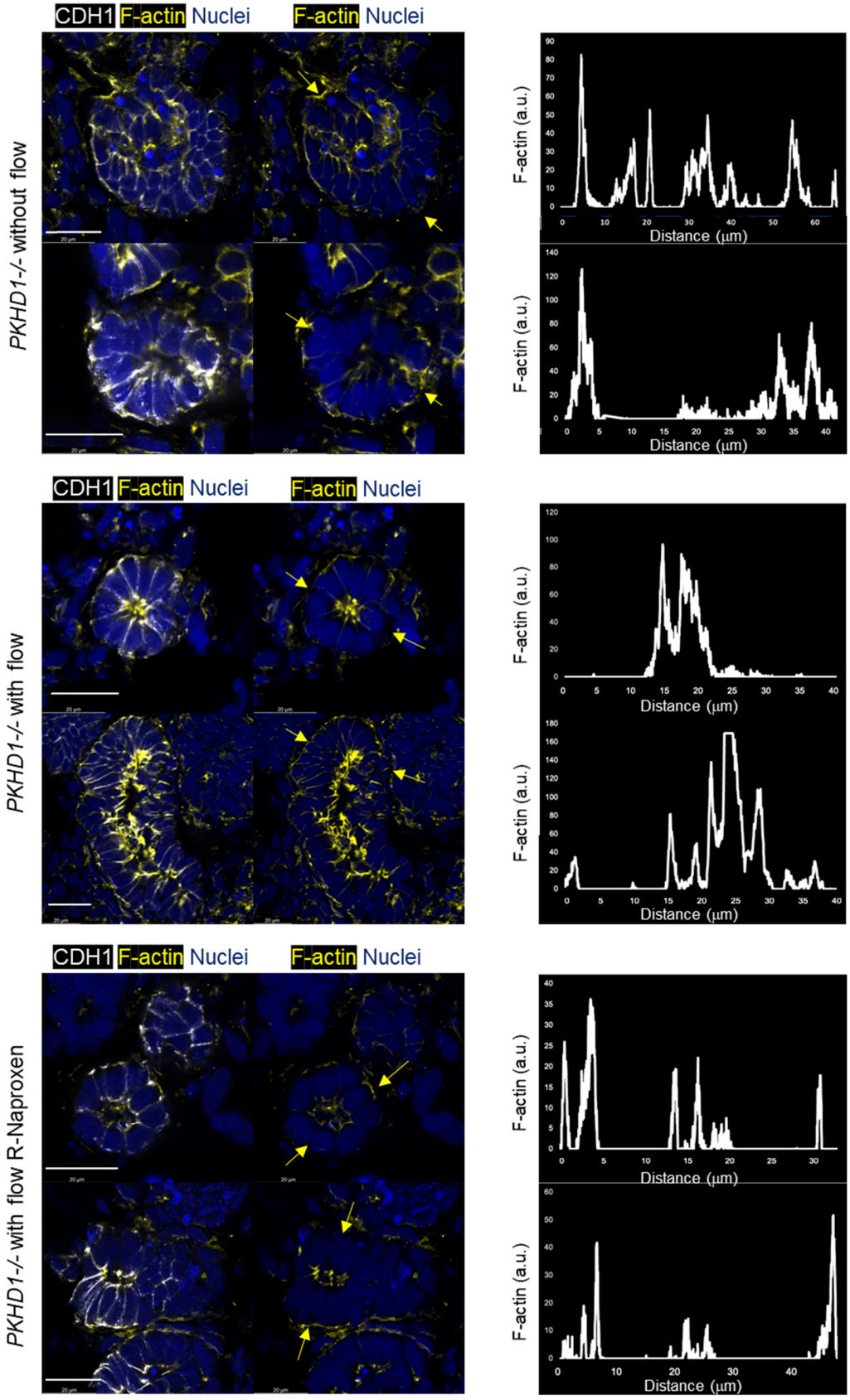

Fig. S18. Immunostaining for CDH1 and F-actin in *PKHD1-/-* organoids. Expression of F-actin and CDH1 in tubules under static, flow, and R-Naproxen treated flow conditions on day 23 of differentiation. Scale bars, 20 μm. The plot profiles of the F-actin intensity across the tubule denoted by yellow arrows are shown on the right.

Fig. S19

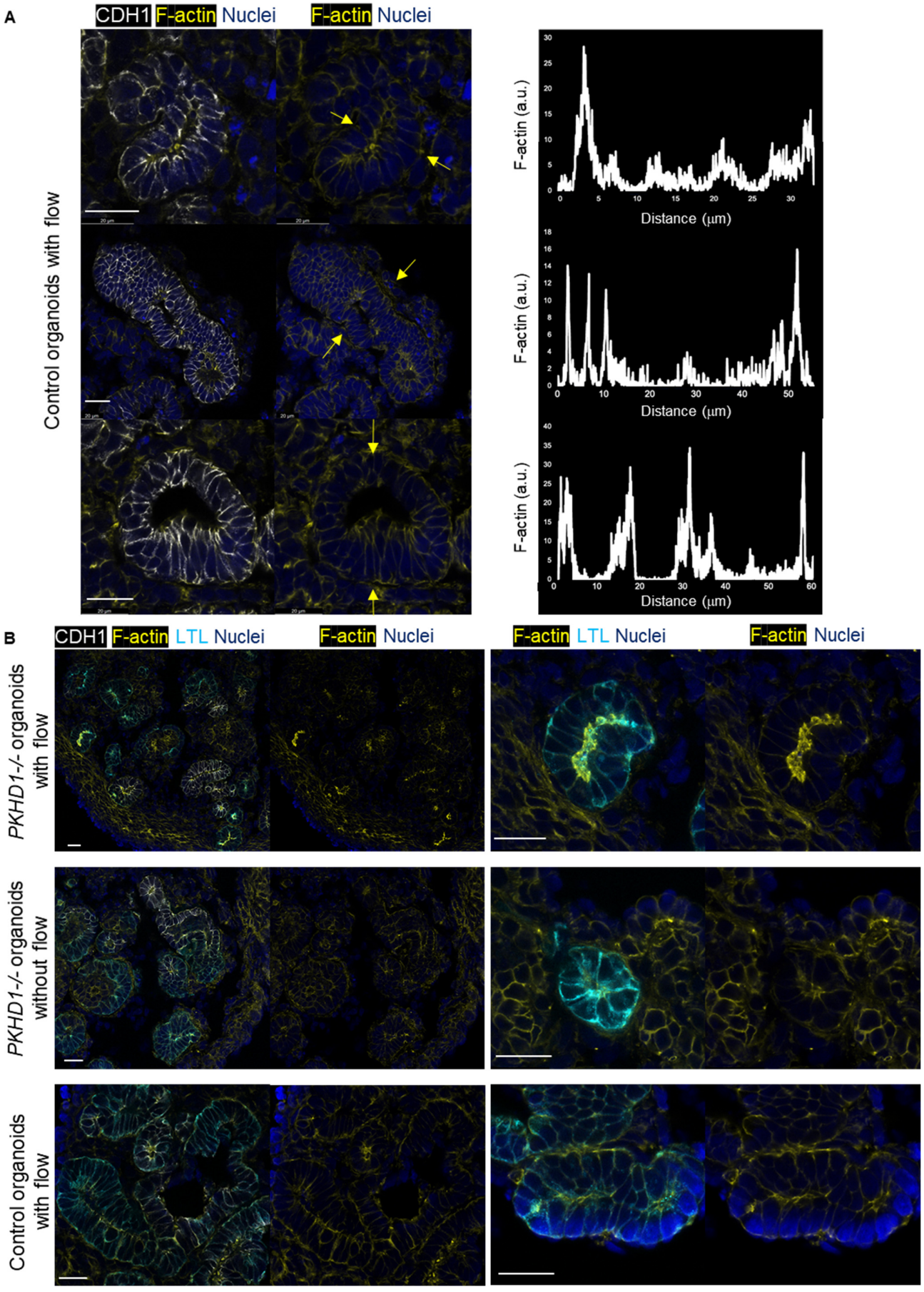
A
CDH1 F-actin Nuclei
F-actin Nuclei
Control organoids with flow
F-actin (a.u.)
Distance (μm)
B
CDH1 F-actin LTL Nuclei
F-actin Nuclei
F-actin LTL Nuclei
F-actin Nuclei
PKHD1-/- organoids with flow
PKHD1-/- organoids without flow
Control organoids with flow

Fig. S19. Immunostaining for segment-specific markers and F-actin in various conditions of organoids. (A) Expression of F-actin and CDH1 in control organoid tubules under flow conditions (n=3) on day 21. Scale bars, 20 μm. The plot profiles of the F-actin intensity across the tubule denoted by yellow arrows are shown on the right. (B) Expression of F-actin, CDH1, and LTL in *PKHD1-/-* organoid tubules under flow conditions on day 23 (upper left). Expression of F-actin and LTL in *PKHD1-/-* proximal tubules under flow conditions on day 23 (upper right). Expression of F-actin, CDH1, and LTL in *PKHD1-/-* organoid tubules in static conditions on day 23 (middle left). Expression of F-actin and LTL in *PKHD1-/-* proximal tubules in static conditions on day 23 (middle right). Expression of F-actin, CDH1, and LTL in control organoid tubules under flow conditions on day 21 (lower left). Expression of F-actin and LTL in control proximal tubules under flow conditions on day 21 (lower right). Scale bars, 20 μm.

Supplementary Table S1. Primer sequences

Gene	Forward	Reverse
RPS18	GCGGCGGAAAATAGCCTTTG	GATCACACGTTCCACCTCATC
DUSP1	GGCCATTGACTTCATAGACTCCA	AACTCAAAGGCCTCGTCCAG
NPTX2	ACGGGCAAGGACACTATGG	ATTGGACACGTTTGCTCTGAG
PRDM1	AAGCAACTGGATGCGCTATGT	GGGATGGGCTTAATGGTGTAGAA
ARFIP2	ATCAGAACGATTTGGTCGAGGC	ATACTTGCGCTTCGTCTCACG
BAIAP2	GACGTATGCAGCCAAAGGCTA	GCAGCTCGTTGTGAAAAGACT